Nanoshells for photothermal therapy: a Monte-Carlo based numerical study of their design tolerance

Thomas Grosges,[1,*] **Dominique Barchiesi,**[1] **Sameh Kessentini,**[1] **Gérard Gréhan,**[2] **and Marc Lamy de la Chapelle**[3]

[1]*Project Group for Automatic Mesh Generation and Advanced Methods - Gamma3 Project (UTT-INRIA) - STMR CNRS UMR 6279, University of Technology of Troyes, 12 rue Marie Curie - BP 2060, 10010 Troyes Cedex, France*

[2]*Complexe de Recherche Interprofessionnel en Aérothermochimie, Université et Institut National des Sciences Appliquées de Rouen, BP 12 - 76801 Saint-Etienne du Rouvray, France*

[3]*CSPBAT CNRS-FRE 3043, UFR SMBH, University of Paris 13, 74 rue Marcel Cachin, 93017 Bobigny, France*

**thomas.grosges@utt.fr*

Abstract: The optimization of the coated metallic nanoparticles and nanoshells is a current challenge for biological applications, especially for cancer photothermal therapy, considering both the continuous improvement of their fabrication and the increasing requirement of efficiency. The efficiency of the coupling between illumination with such nanostructures for burning purposes depends unevenly on their geometrical parameters (radius, thickness of the shell) and material parameters (permittivities which depend on the illumination wavelength). Through a Monte-Carlo method, we propose a numerical study of such nanodevice, to evaluate tolerances (or uncertainty) on these parameters, given a threshold of efficiency, to facilitate the design of nanoparticles. The results could help to focus on the relevant parameters of the engineering process for which the absorbed energy is the most dependant. The Monte-Carlo method confirms that the best burning efficiency are obtained for hollow nanospheres and exhibit the sensitivity of the absorbed electromagnetic energy as a function of each parameter. The proposed method is general and could be applied in design and development of new embedded coated nanomaterials used in biomedicine applications.

OCIS codes: (170.0170) Medical optics and biotechnology; (170.3880) Medical and biological imaging; (290.2200) Extinction.

References and links

1. S. Link and M. A. El-Sayed, "Spectral properties and relaxation dynamics of surface plasmon electronic oscillations in gold and silver nanodots and nanorods," J. Phys. Chem. B **103**, 8410–8426 (1999).
2. J. Aizpurua, P. Hanarp, D. S. Sutherland, M. Kall, G. W. Bryant, and F. J. G. de Abajo, "Optical properties of gold nanorings," Phys. Rev. Lett. **90**, 057401 (2003).
3. Y. G. Sun and Y. N. Xia, "Shape-controlled synthesis of gold and silver nanoparticles," Science **298**, 2176–2179 (2002).
4. S. J. Oldenburg, R. D. Averitt, S. L. Westcott, and N. J. Halas, "Nanoengineering of optical resonances," Chem. Phys. Lett. **288**, 243–247 (1998).
5. C. Loo, A. Lowery, N. J. Halas, J. L. West, and R. Drezek, "Immunotargeted nanoshells for integrated cancer imaging and therapy," Nano Lett. **5**, 709–711 (2005).

#142119 - $15.00 USD Received 2 Feb 2011; revised 22 Apr 2011; accepted 6 May 2011; published 17 May 2011

6. S. R. Sershen, S. L. Westcott, N. J. Halas, and J. L. West, "Temperature-sensitive polymer-nanoshell composites for photothermally modulated drug delivery," J. Biomed. Mater. Res. **51**, 293–298 (2000).
7. D. P. O'Neal, L. R. Hirsch, N. J. Halas, J. D. Payne, and J. L. West, "Photo-thermal tumor ablation in mice using near infrared-absorbing nanoparticles," Cancer Lett. **209**, 171–176 (2004).
8. M. L. Brongersma, J. W. Hartman, and H. A. Atwater, "Electromagnetic energy transfer and switching in nanoparticle chain arrays below the diffraction limit," Phys. Rev. B **62**, 16356–16359 (2000).
9. T. Okamoto, I. Yamaguchi, and T. Kobayashi, "Local plasmon sensor with gold colloid monolayers deposited upon glass substrates," Opt. Lett. **25**, 372–374 (2000).
10. J. B. Jackson, S. L. Westcott, L. R. Hirsch, J. L. West, and N. J. Halas, "Controlling the surface enhanced Raman effect via the nanoshell geometry," Appl. Phys. Lett. **82**, 257–259 (2003).
11. F. Tam and N. J. Halas, "Plasmon response of nanoshell dopants in organic films: a simulation study," Prog. Org. Coat. **47**, 275–278 (2003).
12. S. Link, Z.L. Wang and M.A. El-Sayed, "Alloy formation of gold-silver nanoparticles and the dependence of the plasmon absorption on their composition," J. Phys. Chem. B **103**, 3529-3533 (1999).
13. U. Kreibig and M. Vollmer, *Optical Properties of Metal Clusters* (Springer, 1995).
14. K. L. Kelly, C. Eduardo, L .L. Zhao, and G. C. Schatz, "The optical properties of metal nanoparticles: the influence of size, shape, and dielectric environment," J. Chem. Phys. B **107** (3), 668–677 (2003).
15. E. Prodan and P. Nordlander, "Plasmon hybridization in spherical nanoparticles," J. Chem. Phys. **120**(11), 5444–5454 (2004).
16. D. Barchiesi, E. Kremer, V. P. Mai, and T. Grosges, "A Poincaré's approach for plasmonics: the plasmon localization," J. Microsc. **229**(3), 525–532 (2008).
17. D. Barchiesi, D. Macias, L. Belmar-Letellier, D. van Labeke, M. Lamy de la Chapelle, T. Toury, E. Kremer, L. Moreau, and T. Grosges, "Plasmonics: influence of the intermediate (or stick) layer on the efficiency of sensors," Appl. Phys. B, Lasers Opt. **93**(1), 177–181 (2008).
18. C. Liu, C.C. Mi and B.Q. Li, "Energy Absorption of Gold Nanoshells in Hyperthermia Therapy," IEEE Transactions on Nanobioscience **7**, 206-214 (2008).
19. C. Loo, L. Hirsch, M. H. Lee, E. Chang, J. West, N. Halas, and R. Drezek, "Gold nanoshell bioconjugates for molecular imaging in living cells," Opt. Lett. **30**(9), 1012–1014 (2005).
20. N. K. Grady, N. J. Halas, and P. Nordlander, "Influence of dielectric function properties on the optical response of plasmon resonant metallic nanoparticles," Chem. Phys. Lett. **399**, 167–171 (2004).
21. T. Grosges, D. Barchesi, T. Toury, and G. Gréhan, "Design of nanostructures for imaging and biomedical applications by plasmonic optimization," Opt. Lett. **33**(23), 2812–2814 (2008).
22. C. F. Bohren and D. R. Huffman, *Absorption and Scattering of Light by Small Particles* (John Willey & Sons, Inc., 2003).
23. G. Mie, "Beiträge zur Optik trüber Medien, speziell kolloidaler Metallösungen," Ann. Phys. **25**, 377–445 (1908).
24. G. Gouesbet, B. Maheu, and G. Gréhan, "Light scattering from a sphere arbitrarily located in a Gaussian beam, using a Bromwich formulation," J. Opt. Soc. Am. A **5**, 1427-1443 (1988).
25. C. Gréhan, G. Gouesbet, and F. Guilloteau, "Comparison of the diffraction theory and the generalized lorenz-mie theory for a sphere arbitrarily located into a laser beam," Opt. Commun. **90**, 1–6 (1992).
26. H. Du, "Mie-scattering calculation," Appl. Opt. **43**, 1951–1956 (2004).
27. T. Grosges, A. Vial, and D. Barchiesi, "Models of near-field spectroscopic studies: comparison between Finite-Element and Finite-Difference methods," Opt. Express **13**(21), 8483–8497 (2005), http://www.opticsinfobase.org/oe/abstract.cfm?URI=oe-13-21-8483.
28. D. Barchiesi, B. Guizal, and T. Grosges, "Accuracy of local field enhancement models: toward predictive models?," Appl. Phys. B, Lasers Opt. **84**(1–2), 55–60 (2006).
29. T. Grosges, H. Borouchaki, and D. Barchiesi, "Improved scheme for accurate computation of high electric near-field gradients," Opt. Express **15**(3), 1307–1321 (2007), http://www.opticsinfobase.org/abstract.cfm?URI=oe-15-3-1307.
30. H. Borouchaki, T. Grosges, and D. Barchiesi, "Improved 3D adaptive remeshing scheme applied in high electromagnetic field gradient computation," Finite Elem. Anal. Des. **46**(1–2), 84–95 (2010).
31. E. D. Palik, *Handbook of Optical Constants of Solid I* (Academic Press, 1985).
32. D. Barchiesi and D. van Labeke, "Application of Mie scattering of evanescent waves to scanning optical microscopy theory," J. Mod. Opt. **40**(7), 1239–1254 (1993).
33. D. Macias, A. Vial, and D. Barchiesi, "Application of evolution strategies for the solution of an inverse problem in near-field optics," J. Opt. Soc. Am. A **21**, 1465–1471 (2004).
34. A. M. Schwartzberg, T. Y. Olson, C. E. Talley, and J. Z. Zhang, "Synthesis, characterization, and tunable optical properties of hollow gold nanospheres," J. Phys. Chem. B **110**, 19935–19944 (2006).
35. Z. C. Xu, C. M. Shen, C. W. Xiao, T. Z. Yang, H. R. Zhang, J. Q. Li, and H. J. Gao, "Wet chemical synthesis of gold nanoparticles using silver seeds: a shape control from nanorods to hollow spherical nanoparticles," Nanotechnology **18**, 115608 (2007).
36. D. Barchiesi, "Adaptive non-uniform, hyper-ellitist evolutionary method for the optimization of plasmonic biosensors," in *Proceedings of International Conference on Computers and Industrial Ingineering (CIE39)*, IEEE

#142119 - $15.00 USD Received 2 Feb 2011; revised 22 Apr 2011; accepted 6 May 2011; published 17 May 2011

1, 542–547 (2009).
37. S. Kessentini, D. Barchiesi, T. Grosges, L. Giraud-Moreau, and M. Lamy de la Chapelle, "Adaptive non-uniform particle swarm optimization: application to plasmonic design," Int. J. Appl. Meta. Comput. **2**(1), 18–28 (2011).
38. A. Tarantola, *Inverse Problem Theory and Methods for Model Parameter Estimation* (SIAM, 2005).
39. F. A. Duck, *Physical Properties of Tissue A Comprehensive Reference Book* (Academic Press, 1990).
40. P. Stoller, V. Jacobsen, and V. Sandoghdar, "Measurement of the complex dielectric constant of a single gold nanoparticle," Opt. Lett. **31**(16), 2474–2476 (2006).
41. W. L. Barnes, "Comparing experiment and theory in plasmonics," J. Opt. A, Pure Appl. Opt. **11**, 114002 (2009).
42. L. B. Scaffardi, M. Lester, D. Skigin, and J. O. Tocho, "Optical extinction spectroscopy used to characterize metallic nanowires," Nanotechnology **18**, 315402 (2007).
43. X. Huang and M. A. El-Sayed, "Gold nanoparticles optical properties and implementations in cancer diagnosis and photothermal therapy," J. Adv. Res. **1**(1), 13–28 (2010).

1. Introduction

Extensive theoretical and experimental studies of the interaction between an incident wave with metallic nanostructures, such as nanoparticles, nanodots [1], nanorings [2], nanocubes [3], nanoshells [4], have been achieved in physics and chemistry. Under illumination, these structures, due to local plasmon resonances, are known to exhibit a high enhancement of the electromagnetic field at their surfaces. This field strength depends on the size parameters of the particle and on two related quantities: the wavelength and the permittivity of the used materials (in the case of nanoshell, the core could be made of silica or just a vacuum). Due to this structural tunability of the plasmon resonances, such nanostructures can be of interest in a wide range of applications in biomedicine [5–7].

Therefore, these researches permit to develop applications in nanoscale plasmon waveguide [8] and nanosensing modalities [9–11]. In the past, the choice of the metallic materials and synthesized alloys, size and shape geometries of materials were studied experimentally [12–14] and interpreted as plasmon hybridization [15]. Therefore, the development of metallic nanodevices, where the relative role of electromagnetic and resonant enhancement response could be precisely delineated, necessitates an accurate control of the local electromagnetic field enhancement near the metallic surface [16, 17].

For cancer photothermal therapy, nanodevices like coated metallic nanoparticles and nanoshells are currently used to burn cancer cells. Indeed, most biological tissues have a relatively low light absorption coefficient in the visible (VIS) and near infrared (NIR) regions (600–1300 nm) known as the tissue optical window or therapeutic window. Over this window, organic molecules have limited absorption [18], whereas gold nanodevices, which are biocompatible nontoxic and easily conjugated to antibodies, absorb light millions of times stronger than the organic molecules. Then, almost all the absorbed light is converted to heat via series of nonradiative processes [18] to burn cells in which they are embedded. The plasmon resonance tuning helps to increase the absorbed light and therefore, the nanodevice capability to burn diseased cells.

Until recently, in the absence of optimization of such devices, the absorption efficiency (i.e. the rate of absorbed energy by the particle relatively to the incoming illumination intensity and to the surface of the particle) is only of one order of magnitude [19, 20]. In a recent study, it has been shown that it becomes possible to obtain an absorption efficiency of two order of magnitude in the most convenient wavelength domain for biomedical applications (around 900 nm) [21]. Such a design optimization permits to obtain an increase in the absorption up to two order of magnitude in comparison with the classical coated nanoparticles. However, the sensitivity of such devices to manufacturing uncertainties has never been investigated.

In this study, we focus on the sensitivity design of nanoshells used in photothermal therapy (i.e. the absorption of these particles). The main principle of the method is to select the particles parameters that keep the absorption efficiency greater than a threshold. These parameters are

#142119 - $15.00 USD Received 2 Feb 2011; revised 22 Apr 2011; accepted 6 May 2011; published 17 May 2011

within a range that defines the manufacturing tolerance.

The paper is organized as follows. Section 2 is devoted to the description of the absorption efficiency computation and the requirements on absorption efficiency computation are defined. Then, in section 3, the optimisation scheme by the Monte-Carlo method is presented and explained. The numerical setting related to the considered biomedical application (photothermal therapy for deep cancer using nanoshells) and results will be given and discussed in section 4. Finally, section 5 concludes the paper.

2. Absorption efficiency computation

The total electromagnetic field (near-field and far-field) properties of a metallic nanoobject depends intrinsically on the geometry and on the optical properties of the involved materials. Nanoshells are composed of a core with radius r_1 and of a metallic coating or shell of thickness e (see Fig. 1). The core could be made of silica or just vacuum (the commonly used name of such nanoshells is hollow nanospheres with $n_1 = 1.0$) whereas the shell is made of gold. The permittivity of the core and the permittivity of the coating are denoted ε_1 and ε_2, respectively. The metallic material is characterized by a complex permittivity $\varepsilon_2 = \varepsilon_r + j\varepsilon_i$, (where j^2=-1). The nanoparticles are embedded in a non-absorbing medium with permittivity ε_m, corresponding to biological surrounding. From these parameters (size and permittivities), the electromagnetic field can be computed accurately by a variety of methods, such as analytic Mie scattering theory for spherical geometries [22–26] and numerical methods such as Finite Element Methods (FEM), especially for nanoscale objects of more complex geometries [27–30]. In the following,

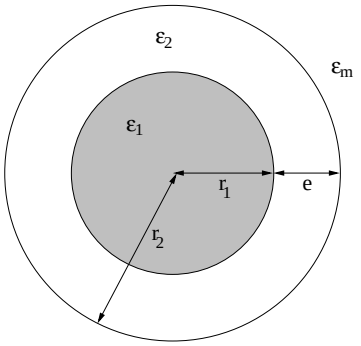

Fig. 1. Nanoshell: inner radius r_1 and shell thickness e.

we compute the absorption efficiency Q_{abs} (see Eq. (3)), which must be maximum to get the more efficient thermal effect. This absorption efficiency can be deduced from W_{abs} which is the rate at which energy is absorbed by the sphere [22]:

$$W_{abs} = \frac{1}{2}\Re\left\{\int_\Omega [\mathbf{E_i}\times\mathbf{H_s^*}+\mathbf{E_s}\times\mathbf{H_i^*}]\,d\Omega\right\} - \frac{1}{2}\Re\left\{\int_\Omega [\mathbf{E_s}\times\mathbf{H_s^*}]\,d\Omega\right\}, \quad (1)$$

where $\mathbf{E_i}$, $\mathbf{H_i}$, $\mathbf{E_s}$ and $\mathbf{H_s}$ are the incident and scattered electric and magnetic components, respectively. The integration is achieved on the solid angle $d\Omega = \rho^2 \sin\theta d\theta d\phi$. It follows that the absorption cross section is defined by:

$$C_{abs} = \frac{W_{abs}}{I_i} = \frac{2\pi}{k^2}\sum_{n=1}^{\infty}(2n+1)\left\{\Re[a_n+b_n] - \left[|a_n|^2+|b_n|^2\right]\right\}, \quad (2)$$

#142119 - $15.00 USD Received 2 Feb 2011; revised 22 Apr 2011; accepted 6 May 2011; published 17 May 2011

where I_i is the incident intensity, $k = 2\pi\sqrt{\varepsilon_m}/\lambda$ being the wave vector in the surrounding medium, and a_n and b_n are the scattering coefficients. The absorption efficiency Q_{abs} is therefore the absorption cross section C_{abs} per unit of area $S = \pi(r_1 + e)^2$:

$$Q_{abs} = \frac{C_{abs}}{S} = \frac{2}{k^2(r_1+e)^2}\sum_{n=1}^{\infty}(2n+1)\left\{\Re\left[a_n + b_n\right] - \left[|a_n|^2 + |b_n|^2\right]\right\}. \quad (3)$$

In the limit of small particles ($r_2/\lambda << 1$) [22], the computation of Q_{abs} is often achieved by neglecting the order $n > 1$ in the expansion of the series (Eq. (3)) [22]. Therefore, in the limit of small particle approximation, the dipolar approximation consists in considering only the a_1 and b_1 (called dipolar electric and magnetic) terms of the series in Eq. (3). In the present study, the question is: is this dipolar approximation valid for the considered nanoshells (i.e. limiting the Q_{abs} computation with n=1)?

We show in Fig. 2 that even for small particles as nanoshells, this dipolar approximation is not valid. We summary in Table 1 the acceptable intervals of parameters for inner radius r_1, thickness e, illuminating wavelength λ and the relative real and imaginary parts of the bulk permittivity of gold $\varepsilon_2(\lambda)$ [31]. Figures 2(a) and 2(b) show the relative error between the absorption efficiency Q_{abs} computed from the dipolar approximation and the series (Eq. (3)), with 60 terms, ensuring a convergence of the series, better than 10^{-12}). The ratios of the radius to the wavelength are $r_2/\lambda = 0.092$ and $r_1/\lambda = 0.089$ (Fig. 2(a)), and $r_2/\lambda = 0.022$ and $r_1/\lambda = 0.021$ (Fig. 2(b)). Even if the computation is based on the systematic variation of the permittivity of the gold shell within the domain of wavelengthes of $[800;1000]$ nm, the external radius of the nanoshell is between $800 \times 0.092 = 73.6$ nm and $1000 \times 0.092 = 92$ nm and the relative error is greater than 25% (see Fig. 2(a)). The relative error cannot be neglected in both cases.

Table 1. Summary of Acceptable Intervals of Parameters r_1, e, λ, $\varepsilon_r(\lambda)$ and $\varepsilon_r(\lambda)$

Parameters	
inner radius r_1 (nm)	[1.0; 150.0]
shell thickness e (nm)	[1.0; 50.0]
wavelength λ (nm)	[800; 1000]
$\varepsilon_r(\lambda)$	[-42.0; -23.0]
$\varepsilon_i(\lambda)$	[1.5; 3.0]

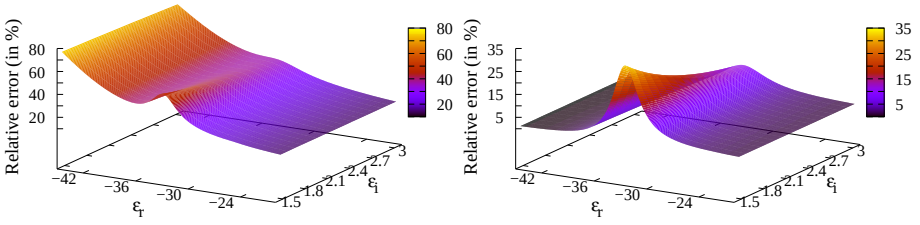

(a) (b)

Fig. 2. Relative error between the exact computation of Q_{abs} and its approximation in the small particle limit for radii, as a function of the real ε_r and imaginary part ε_i of the material permittivity for particle radii: (a) $r_1/\lambda = 0.089$ and $e/\lambda = 0.003$, (b) $r_1/\lambda = 0.021$ and $e/\lambda = 0.001$.

#142119 - $15.00 USD Received 2 Feb 2011; revised 22 Apr 2011; accepted 6 May 2011; published 17 May 2011

This result shows that the computation of Q_{abs} with dipolar approximation is not appropriate even for small particles with thin gold coating (see Fig. 2(b)). In the case of the present study, the series of the efficiency cannot be limited to the first order and the dipolar approximation is not relevant. The dipolar approximation cannot be used for the prediction of the location of plasmon resonance and therefore for optimization in the biological window [32].

Therefore, for sensitivity design, the multipolar computation of Q_{abs} must be achieved (i.e. more than one term must be computed in the series). In the following, the computations of the Q_{abs} are achieved by using the full Mie's theory (i.e. the series of Eq. (3) are computed with 60 terms, ensuring a convergence of the series, better than 10^{-12}). In the next section, we introduce the computational Monte-Carlo method used to compute the sensitivity of the absorption efficiency Q_{abs} to the various parameters of the problems. The tolerances for each parameter will be deduced, so that Q_{abs} remains above a given threshold.

3. The adaptive Monte-Carlo method

The main purpose is to determine the parameters of the nanoparticles that are critical for medical application. For this, we introduce a boundary adaptive method based on a Monte-Carlo scheme. The proposed approach differs strongly from the metaheuristic optimization algorithms we applied in the previous studies, either to the inverse problem solving in near-field optics [33], or to optimize the Surface Plasmon Resonance planar biosensor [17, 34–37]. In those papers, the goal was to compute the best set of parameters to get the most efficient biosensor. Nevertheless, no propagation of uncertainty has been determined, despite the known uncertainties on permittivities and geometrical parameters. Recently, we have proposed a method to design the nanoshells with silica core for imaging and burning applications [21]. In that study, an evolutionary method (i.e. developping similar operational principles based on the evolution of the searched parameters as objective variables to reach a target) was used to optimize the size parameters and the permittivity of the shell using existing permittivities. However, the optical index of the core was fixed to that of silica (which is not the case in this study). The goal was to obtain at least 80% of the mathematical maximum of the absorption Q_{abs} (resp. scattering) efficiency, for the burning (resp. imaging) purpose. This method is now used to find the best set of parameters to reach $max(Q_{abs})$ without fixing the optical index of the core nor the wavelength.

Otherwise, in the present paper, the proposed method consists in fixing a tolerance on the optimum of the absorption efficiency, to determine a class of acceptable parameters. Then, the tolerance on the various parameters can be deduced and interpreted either in terms of sensitivity of the model or acceptable uncertainty in the process of fabrication. For this, a family of parameters of the nanoshells (size and permittivities) is randomly generated, and the algorithm retains the maximal and minimal values (i.e. the boundaries) of the parameters for which the efficiency remains greater than a given fraction α of the optimal efficiency. The process is repeated (by regenerating randomly another set of nanoshells given the new boundary constraints and looking for additional "good" nanoshells) until a given number of "good" nanoshells are obtained and analyzed to depict the sensitivity to each size or optical parameter. This approach is derived from a classical metaheuristic engineering approach of the study of uncertainties propagation through a numerical model of the system, to compute the engineering tolerances. Actually, the Monte-Carlo method relies on repeated random sampling to compute their results (e.g. probability of fitting some conditions) in a fixed domain (or boundaries) given usually by physical constraints. It is known to be an effective substitute to the traditional method of experimental plan, indeed to solve inverse problems [38].

In this paper, we present the method permitting to compute the intervals of optimized size parameters and core index that guarantee absorption efficiency Q_{abs}, given an acceptable percentage α of its maximum. This maximum absorption efficiency $\max(Q_{abs})$ is corresponding

#142119 - $15.00 USD Received 2 Feb 2011; revised 22 Apr 2011; accepted 6 May 2011; published 17 May 2011

to the theoretical maximum best absorption efficiency obtained for the optimized size and materials parameters. This maximum is computed with Eq. (3) and the best parameters are determined through the evolutionnary method [21]. Therefore, the target of the problem is finding a family $\mathbf{p}$ of the optical and of the size parameters for the nanoshell, that enables to maintain $Q_{abs}(\mathbf{p}) > \alpha \max(Q_{abs})$. The family of parameters is $\mathbf{p} = [r_1, e, \lambda, \varepsilon_1, \varepsilon_2(\lambda)]$, where r_1 is the radius of the core, e is the thickness of the metal coating (shell), λ is the illumination wavelength, ε_1 the permittivity of the core and $\varepsilon_2(\lambda)$ the permittivity of the gold shell. The permittivity of the external medium is ε_m.

3.1. Principle of the method of model sensitivity study

This numerical method is summarized as following, considering a threshold $\alpha = 90\%$, delineating an acceptable value of Q_{abs}:

1. Define an initial domain of possible parameters (size parameters r_1^0 and e^0 and permittivities ε_1^0, $\varepsilon_2^0(\lambda)$) by setting the boundaries according to physical constraints. The number of parameters set *npt* is fixed as the maximum of the domain of variation of the initial parameters divided by their uncertainty u in the process of fabrication [38]: $npt = \max\left\{[\max(r_1^0) - \min(r_1^0)]/u(r_1);\ [\max(e^0) - \min(e^0)]/u(e);\ [\max(n_1^0) - \min(n_1^0)]/u(n_1);\ [\max(\lambda^0) - \min(\lambda^0)]/u(\lambda)\right\}$. Within the range of parameters, the maximum of Q_{abs} is computed with the above mentioned evolutionary method [21].

2. Random generation of a family of *npt* unknown parameters sets $\mathbf{p}(t)$, using uniform laws in the considered domain. t is the iteration index initially set to 1.

3. Computation of the optimum geometrical parameters with Nelder-Mead method: this method requires an initial values for the optimum search. These initial values are the parameters set that gives the maximum value $\max_t(Q_{abs})$, within the family: $[r_1, e, \lambda, \varepsilon_2(\lambda)]$, ε_1 being unchanged. This maximum is $\max_{NM}(Q_{abs})$, and varies slightly with t. Actually, the basic Nelder-Mead method is a multidimensional unconstrained nonlinear method that cannot handle with boundaries in the search domain and therefore, if n_1 would be also a parameter to be optimized, the output of the algorithm would give $n_1 = 0$, which is not compatible with the physical constraint on the optical index of a dielectric medium $n_1 \geq 1$. The optimum set generated by this method will be denoted $p_{max}(t)$ and the corresponding absorption efficiency $\max_{NM}(Q_{abs})$.

4. Selection and storage of the best parameters sets of the family $\mathbf{p}(t)$ for which $Q_{abs} > \alpha \max_{NM}(Q_{abs})$. The retained sets form a family denoted $\mathbf{p}_\alpha(t)$. The set $p_{max}(t)$ is not added to this family $\mathbf{p}_\alpha(t)$ but is used only to determine $\max_{NM}(Q_{abs})$.

5. Updating boundaries of the domain using the minimum and the maximum of each parameter in $\mathbf{p}_\alpha(t)$.

6. Increment t and loop on step 2, until the size of all the selected sets of parameters $\bigcup_t \mathbf{p}_\alpha(t)$ is greater than *npt*. The final number of iteration is N_t.

The associated tolerance in fabrication will be deduced from the boundaries of this last family.

3.2. Benchmark of the adaptive Monte-Carlo sensitivity study

At this stage, two points should be clarified. First, the advantage of the adaptive method v.s. the classical Monte-Carlo method. To reach an accuracy on the boundaries determination lower than 1%, the number of random parameters should be greater than $100,000$, the convergence of

#142119 - $15.00 USD Received 2 Feb 2011; revised 22 Apr 2011; accepted 6 May 2011; published 17 May 2011

the classical Monte-Carlo method being in $1/\sqrt{npt}$. The advantage of our adaptive method lies in the adaptation of the domain of search, keeping constant the number of random parameters at each iteration, from a generation to the following. Therefore the convergence is better at each new iteration and the precision on the boundaries is increased.

Second, the numerical cost of the method has to be compared to the cost of the four loops required in a systematic study. For this, we use the numerical parameters, that are physically acceptable for the initialization of the algorithm. We consider $r_1 \in [1;100] = [\min(r_1^0);\max(r_1^0)]$ nm; $e \in [1;50]$ nm as small particles are preferred in burning applications.

For the benchmark of the algorithm, we used the same parameters as in Ref. [21] where non heuristic method was used to compute the tolerance on the parameters. Table 2 shows the various parameters of the study and the obtained results. In that study the optical index of the silica core (resp. external medium) was $\varepsilon_1 = 2.4$ (resp. $\varepsilon_3 = 1.77$). For illustration, we focus on a specific result for gold nanoshell and $\lambda = 850$ nm. The threshold was $\alpha = 80\%$. The

Table 2. Benchmark of the Adaptive Monte-Carlo Model Sensitivity Study: Comparison with Systematic Study [21]

Parameters	Ref. [21]	Monte-Carlo
inner radius r_1 (nm)	25.1 ± 9.8	$[16.7(0.6);30.2(0.6)]$
shell thickness e (nm)	3.0 ± 1.3	$[1.9(0.1);3.9(0.1)]$
$\max_{NM}(Q_{abs})$	11.6	11.6
best r_1 (nm)	25.1	24.7
best e (nm)	3.0	2.9
Number of Q_{abs} evaluations	$24,000$	6700

*The maximum of the efficiency is deduced from Table 2 in Ref. [21] and the reference by Loo et al. [5]: $11.6 = 0.144 \times 80.2$. The number of evaluations is that required for permittivity choice as well as optimization of the geometry of the nanoshell: $20,000 + 4,000$ [21]. For the Monte-Carlo method, the standard deviation of the boundaries across the iterations is also indicated between parenthesis.

computation of the standard deviation of the boundaries obtained for all iterations can be held as an indicator of the confidence on the computed boundaries. Indeed, the standard deviation of the boundaries can be considered as uncertainty and is an indicator for limiting the significative digits of the results. Increasing npt results in a $1/\sqrt{npt}$ decreasing of the standard deviations of the boundaries, the number of iterations being almost constant (N_t around 40).

The Monte-Carlo method, gives the tolerance on the radius r_1 and the thickness e. These tolerances are deduced from the intervals of acceptable values of each parameter. The tolerances correspond to those obtained from a systematic study like experience plane [21], but the number of required evaluations of Q_{abs} is reduced. The computational scheme requires less than 40 iterations (with 990 evaluations of Q_{abs}) and therefore, less than 40,000 evaluations of Q_{abs}, while a three loops systematic study would require $990 \times 49 \times 200 \approx \times 10^7$ evaluations [21].

These results are validating the Monte-Carlo approach which helps to compute sensitivity of the model to the input parameters. From Table 2, we can deduce that the critical parameter is the thickness of gold, the tolerance on r_1 being around four times greater. After convergence of the Monte-Carlo scheme, the boundaries of the last hypercube can be used to define the tolerance on each parameter.

A last bench has been made before the use of this method for more general problems. Indeed, it is well known that the reiteration of metaheuristic methods has to be made to characterize stability and dispersion of the results. Thousand realizations of the proposed Monte-Carlo code, with different initializations of the random generator, have been made to check the stability of

#142119 - $15.00 USD Received 2 Feb 2011; revised 22 Apr 2011; accepted 6 May 2011; published 17 May 2011

the algorithm. The obtained results show a standard deviation of the boundaries, over the thousand realizations, which is smaller than the initial tolerance on each parameter. Therefore, the method could be applied with sufficient confidence to the sensitivity design of nanoshells. Let us investigate the case of hollow nanoshells ($n_1 \approx 1$) and coated silica ($n_1 = 1.54$) nanospheres in fat instead of water [39].

4. Sensitivity design of nanoshells for photothermal therapy

4.1. Sensitivity of the model with free optical index of the core

We focus on the design of gold coated nanoparticles (or nanoshells) for applications in the biomedical domain of wavelengths ($\lambda \in [800;1000]$ nm), for cell burning purpose. The control of absorption efficiency by tuning the wavelength and the size in visible and infrared region has been proved experimentally [19, 34]. Nevertheless, the optical constant of gold nanoparticles is not known exactly. Moreover, strong variations have been found for bulk and obviously for thin layers, depending on the mode of deposition. With such variations in the values of the permittivity for gold, the question is: is the numerical optimization using the bulk permittivity for the gold shell adapted? In fact, despite the variations between values of the permittivity for gold nanoparticles and bulk values, the results of computation of cross sections are in good agreements with experiment results, especially in the case of spectroscopic studies of such nano-devices [40–42]. Hopefully the following results confirm that the geometrical parameters are more critical in the design than the optical index of gold.

The permittivity of the core $\varepsilon_1 \in [1;16]$ as the commonly used core is made of silica or vacuum (with vacuum core, the corresponding nanoshells are commonly known as hollow nanospheres). The uncertainty on the optical core index $n_1 = \sqrt{\varepsilon_1}$ is fixed to 0.01. The permittivity of the gold coating (or shell) is obtained from the Palik's data [31], in the $[800;1000]$ nm range of wavelength λ: $\varepsilon_2(\lambda)$. Therefore, the real part of the gold permittivity lays between -42 and -24. The imaginary part of this permittivity is between 1.5 and 3. A fit of this permittivity with λ's step equal to 1 nm is used. On the contrary of Ref. [21], the material of the shell is fixed and our results reveal the shallow sensitivity on this parameter.

Let us investigate first the most general case, where the index of the core must also be determined, the initial set of parameters is summarized in Table 3. Therefore,

Table 3. Parametric Setting: Domain and Accuracy

Parameters	Domain	uncertainty u
inner radius r_1 (nm)	[1; 100]	0.1
shell thickness e (nm)	[1; 50]	0.1
illumination wavelength λ (nm)	[800; 1000]	1
core optical index $n_1 = \sqrt{\varepsilon_1}$	[1; 4]	0.01

the size of each family of parameters at each iteration, npt, can be evaluated: $npt = \max\{(100-1)/0.1,(50-1)/0.1,(1000-800)/1,(4-1)/0.01,(800-400)/1\} = 990$.

In the following, we present the histograms for each parameter (see Fig. 3). These results are obtained for a value of Q_{abs} which falls within the interval $[0.9\max_{NM}(Q_{abs});\max_{NM}(Q_{abs})]$. At this stage, the determination of the tolerance on experimental parameters can be evaluated: it is actually the size of the last domain [38] (i.e. the minimum and maximum on the x-axis of each histogram). The boundaries of this domain can be considered as an absolute confidence interval of the parameters for the threshold α (all parameters within this interval product acceptable efficiency). Nevertheless, the visual inspection of each histogram in Fig. 3 enables the

#142119 - $15.00 USD Received 2 Feb 2011; revised 22 Apr 2011; accepted 6 May 2011; published 17 May 2011

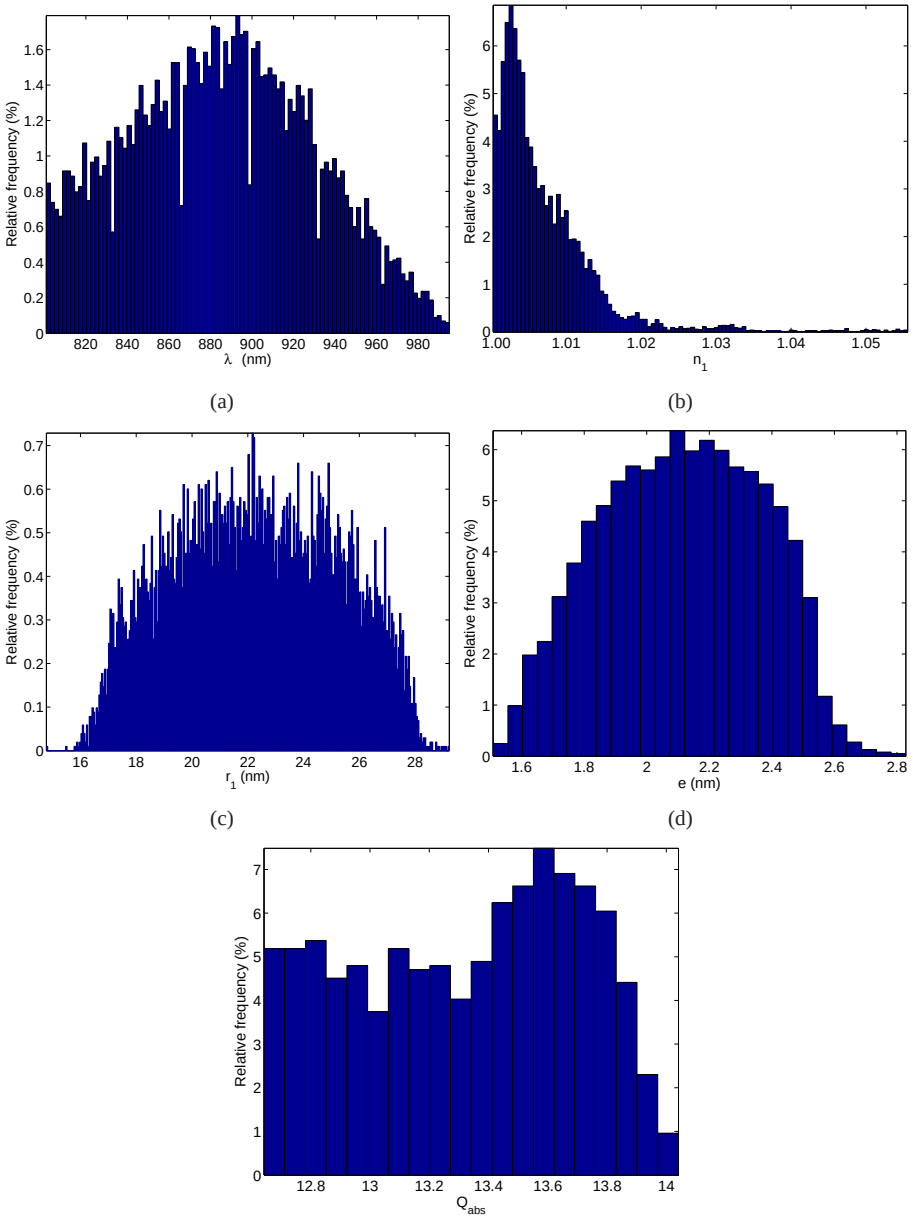

Fig. 3. Histograms of (a) the wavelength, (b) the optical index of the core ($n_1 = \sqrt{\varepsilon_1}$) (c) the radius of the core, (d) the thickness of the shell, (e) the absorption efficiency. The relative frequency is plotted in percents, and the number of class is deduced from the uncertainty in Table 3, except for the absorption efficiency where the size of each class is fixed to $0.5\% \max_{NM}(Q_{abs})$.

#142119 - $15.00 USD Received 2 Feb 2011; revised 22 Apr 2011; accepted 6 May 2011; published 17 May 2011

classification of each parameter in terms of sensitivity of the result. The conclusions are:

- hopefully, the sensitivity of Q_{abs} to the wavelength (and consequently to the permittivity of gold) is low. In the investigated range of wavelengthes ($[800;1000]$ nm), the permittivity has monotonic variations. Therefore the nanoshell can be efficient in this whole domain of wavelengthes. Moreover, the exact knowledge of permittivity of the shell seems not to be critical. This behavior can be explained by the broadening of the multipolar resonance of the nanoshell due to the non negligible imaginary part of the permittivity.

- The less the inner permittivity is, the better is the efficiency of the nanoshell (see Fig. 3(b) with $n_1 \approx 1.0$ and Fig. 3(e) with $12.7 \leq Q_{abs} \leq 14.0$). This confirms that the hollow nanosphere seems to be the more efficient. Schwartzberg *et al.* have shown that the absorption band of these particles can be tuned by adjusting the thickness of the gold shell and the inner radius and thus would enable both strong scattering and absorption efficiency [34].

- The computed tolerances on radii are within these of fabrication processes (0.6 nm [34, 35]). But the thickness of the gold shell is the most critical parameter: $e = 2.1 \pm 0.6$. $r_1 = 22.5 \pm 6.5$ and the best parameters are $r_1 = 22.2$ nm, $e = 2.0$ nm, to get $\max_{NM}(Q_{abs}) = 14.0$. The best parameters for λ, r_1 and e are close the center of the intervals of tolerance and $n_1 \approx 1.0$. The standard deviation of the boundaries of intervals are respectively 0.5 for r_1, 0.05 for e and 10^{-3} for n_1. These values are around ten times lower than the size of each interval, ensure the validity of the above intervals of tolerance, and confirm the sensitivity of Q_{abs} to each parameter. In particular, the high sensitivity of Q_{abs} to the thickness of gold is observed and can be assimilated to the same behavior observed for Surface Plasmon Resonance based planar biosensors [17].

- The histogram of Q_{abs} shows a maximum of 14.0 and of course a minimum of 12.9 which is related to the threshold $\alpha = 0.9$.

With such parameters, the absorption efficiency, relatively to the reference particle size (see Loo et al. [19]), corresponds to a gain of 60 to 100.

Figures 4(a)–4(d) show the convergence of the boundaries of the domain. In this case, the maximum number of iterations required to get at least *npt* parameters sets $\bigcup_t \mathbf{p}_\alpha(t)$ satisfying the target $Q_{abs}(\mathbf{p} \in [0.9 \max_{NM}(Q_{abs}); \max_{NM}(Q_{abs})])$ is $N_t = 30$. It illustrates the rapid convergence of the boundaries which can be considered as the tolerance on each parameter, and their low dispersion. The minimum and the maximum of the wavelength (not shown here) remain the same along the iterations. Figures 4(a)–4(c) show the quick convergence of n_1 toward unity, and of the shell thickness in a small interval compared to the initial one. Clearly, the sensitivity of Q_{abs} to r_1 is less. Figure 4(d) shows that the maximum of absorption among the family $\mathbf{p}_\alpha(t)$ (diamonds) and the best solution $p_{max}(t)$ determined by Nelder-Mead optimization (plus), are close together ($max(Q_{abs}) \approx 14$) since iteration 20. This confirms that the space of parameters search is therefore reduced efficiently.

4.2. Sensitivity of the model with silica core

A second application is carried to study one of the commonly manufactured nanoparticles: the nanoshells with silica core. For this, the optical index n_1 is fixed to 1.54. This is possible as its variation with the wavelength within the range $[800;1000]$ nm is negligible. The proposed Monte-Method results are $r_1 \in [18.2(0.6); 28.2(0.6)]$ nm and $e \in [2.1(0.06); 3.3(0.06)]$ nm. The standard deviation of each boundary in the family $\bigcup_t \mathbf{p}_\alpha(t)$ of 990 acceptable parameters is indicated in parenthesis. The tolerance on the geometrical parameter is of the same order

#142119 - $15.00 USD Received 2 Feb 2011; revised 22 Apr 2011; accepted 6 May 2011; published 17 May 2011

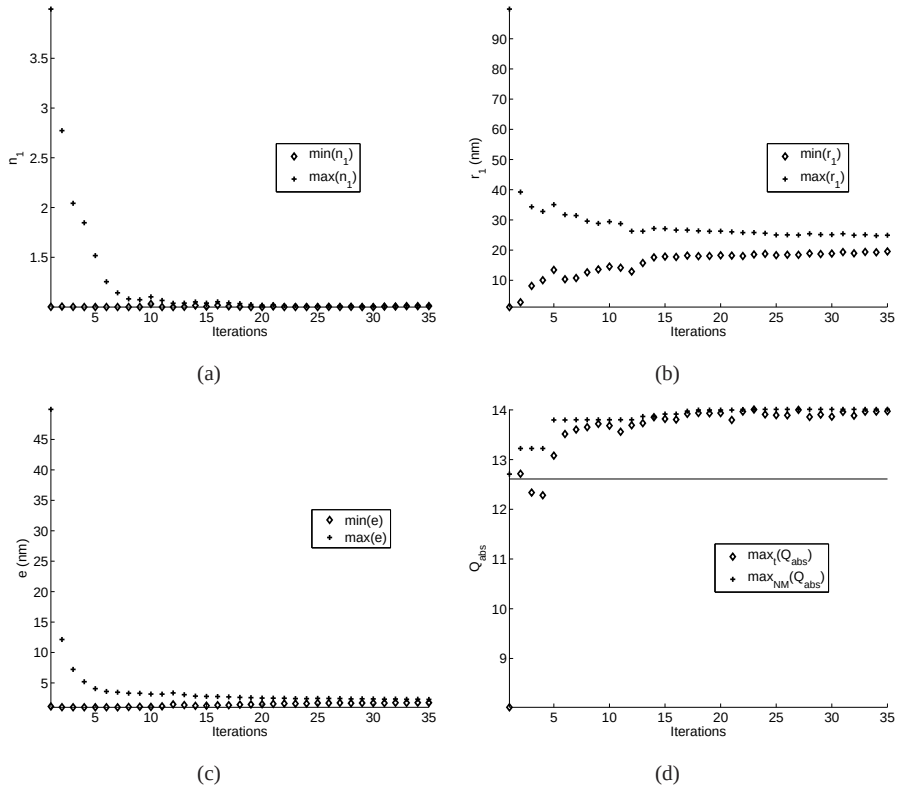

Fig. 4. Example of the convergence of the boundaries as a function of the iterations: (a) the optical index of the core ($n_1 = \sqrt{\varepsilon_1}$) (b) the radius of the core, (c) the thickness of the shell, (d) the absorption efficiency. The minimum and the maximum for each parameter for the last iteration are the final results. The plot of the convergence of the wavelength is useless since its interval remains almost the same at each iteration.

of that in the previous subsection, and the best values are comparable. Therefore, the core index n_1 of the nano-shell can be considered as much less critical than the thickness of gold e. These results are confirmed if we decrease the threshold of tolerance to $\alpha = 50\%$. In this case, $r_1 \in [9(1);46(1)]$ nm and $e \in [1.0(0.2);5.9(0.2)]$ nm.

Moreover, $\max_{NM}(Q_{abs}) = 12.2$ for $r_1 = 23.2$ nm and $e = 2.7$ nm and therefore, the best efficiency of the coated particle is hardly smaller than $0.9\max_{NM}(Q_{abs})$ for hollow spheres. This result shows that the gold coated spheres may continue to be used to burn cancer cells. This low loss of efficiency should not prevent their use for their lesser fragility. Nevertheless, the control of the thickness of the coating and its quality should be improved mainly as forming a uniform shell on the silica core is very difficult for small clusters [43].

5. Conclusion

We proposed an iterative Monte-Carlo method with boundary adaptation, to compute the sensitivity of the absorption efficiency of nanoparticles. The goal was to determine the sensitivity of the geometrical and material parameters, that could maintain a sufficiently high absorption efficiency, to get an elevation of its temperature for burning purposes. The proposed algorithm

#142119 - $15.00 USD Received 2 Feb 2011; revised 22 Apr 2011; accepted 6 May 2011; published 17 May 2011

enables to spare evaluations of the target (Q_{abs}) with regards to a systematic study, through simple loops. The obtained results are coherent with former experimental and theoretical results and are statistically significant. In particular, the method shows that the hollow nanoshells (no material in the core) are more efficient. The extent of the domain of possible parameters shows that the shell should be synthesized with more precision to guarantee a maximal absorption. On the other hand, the efficiency of the nanoparticles also depends on the gold process of deposition and on the inner radius. The method introduced in this study is general and can be applied to a wide range of problems and especially to nanoparticles in order to obtain an optimized design of the size, the shape, the geometry and to select the most adapted for a specific application. The extension to non-spherical particles with complex geometry may give perspectives for both research and applicative purposes, especially in the optical imaging and in the biomedical domain. The extension to complex or non-spherical geometries will necessitate the definition of additional geometrical parameters (like roughness), the development of an adapted numerical method (e.g. FEM, DDA,..) to compute the target to optimize (Qabs, or absorbed enery) for the considered geometry. Nevertheless, this study opens a way in the easier manufacturing and development of a new family of sophisticate nanostructures (nanoshells, nanorings, nanodots, etc.) with optimized design.

Acknowledgments

Authors thank the Centre de Calcul Intensif ROMEO2 for computational facilities, the Région Champagne-Ardennes, the Conseil Régional de l'Aube and the *Nanoantenna* European Project (FP7 Health-F5-2009-241818) for financial supports.

#142119 - $15.00 USD Received 2 Feb 2011; revised 22 Apr 2011; accepted 6 May 2011; published 17 May 2011